0013-7227/02/$15.00/0
Printed in U.S.A.

Endocrinology 143(7):2469–2477

Targeted Disruption of the Melanin-Concentrating Hormone Receptor-1 Results in Hyperphagia and Resistance to Diet-Induced Obesity

YANYUN CHEN, CHANGZHI HU, CHIUN-KANG HSU, QING ZHANG, CHEN BI, MARK ASNICAR, HANSEN M. HSIUNG, NILES FOX, LAWRENCE J. SLIEKER, DEREK D. YANG, MARK L. HEIMAN, AND YUGUANG SHI

Division of Endocrinology (Y.C., C.H., C.-K.H., C.B., M.A., H.M.H., L.J.S., M.L.H., Y.S.), Division of Bio-Research Technologies and Proteins (Q.Z., N.F., D.D.Y.), Lilly Research Laboratories, Eli Lilly & Co., Indianapolis, Indiana 46285

The hypothalamic neuropeptide melanin-concentrating hormone (MCH) has been implicated in a variety of physiological functions including the regulation of feeding and energy homeostasis. Two MCH receptors (MCHR1 and MCHR2) have been identified so far. To decipher the functional role of the MCH receptors, we have generated and phenotypically characterized mice rendered deficient in *MCHR1* expression by homologous recombination. Inactivation of *MCHR1* results in mice (*MCHR1*−/−) that are resistant to diet-induced obesity. With a high-fat diet, body fat mass is significantly lower in both male (4.7 ± 0.6 g *vs.* 9.6 ± 1.2 g) and female (3.9 ± 0.2 *vs.* 5.8 ± 0.5 g) *MCHR1*−/− mice than that of the wild-type control ($P < 0.01$), but the lean mass remains constant. When normalized to body weight, female mice are hyperphagic, and male mice are hyperphagic and hypermetabolic, compared with wild-type mice. Consistent with the lower fat mass, both leptin and insulin levels are significantly lower in male *MCHR1*−/− mice than in the wild-type controls. Our data firmly establish MCHR1 as a mediator of MCH effects on energy homeostasis and suggest that inactivation of *MCHR1* alone is capable to counterbalance obesity induced by a high-fat diet. (*Endocrinology* 143: 2469–2477, 2002)

MELANIN-CONCENTRATING HORMONE (MCH), a cyclic neuropeptide that regulates skin color in teleost fish, was originally isolated from the salmon pituitary (1). Mammalian MCH is predominantly expressed in the lateral hypothalamus and zona incerta with extensive projection throughout the brain (2, 3). The expression pattern of MCH suggests that it plays a role in the regulation of energy balance. The hypothalamic MCH mRNA level is up-regulated in leptin-deficient (*ob/ob*) mice and further increased by fasting (4). Centrally administered MCH stimulates food intake (4, 5). MCH-deficient mice are hypophagic and hypermetabolic with decreased body weight and increased leanness (6), but overexpression of MCH in mice leads to obesity and insulin resistance (7). These results indicate that MCH is involved in the regulation of feeding and energy metabolism. MCH has also been implicated in a variety of physiological functions including regulation of hypothalamic-pituitary-adrenal axis (8) as well as regulation of reproduction (9, 10), memory (11), and motivational behavior (12). These diverse functions may be mediated by multiple MCH receptors.

An orphan G protein-coupled receptor, SLC1/GPR24, was identified as an MCH receptor (MCHR1) in 1999 (13, 14). MCHR1 is widely expressed in multiple regions of the brain including cortex, hippocampus, thalamus, midbrain, pons, olfactory bulb, and hypothalamus (15, 16). MCHR2 was identified recently on the basis of the sequence homology to MCHR1 (17–20). The expression pattern of both receptor isoforms in the brain is similar, although MCHR2, unlike MCHR1, is not expressed in the pituitary (18). In particular, MCHR1 and MCHR2 are expressed in the hypothalamic areas such as the ventromedial, dorsomedial, and arcuate nuclei implicated in the control of energy homeostasis (19). To gain insight of the functional role of the MCHRs, we created a mouse model of MCHR1 deficiency by disrupting the *MCHR1* gene locus using homologous recombination in embryonic stem cells. Homozygous *MCHR1*−/− mice exhibit hyperphagia and resistance to diet induced by obesity. Thus, MCHR1 appears to play an important role in the regulation of energy homeostasis mediated by MCH.

Abbreviations: BAC, Bacterial artificial chromosome; ES, embryonic stem; MCH, melanin-concentrating hormone; MCHR1 and MCHR2, MCH receptor 1 and 2; *MCHR1*−/−, homozygous MCHR1 knockout mice; NEI, neuropeptide EI; POMC, proopiomelanocortin; RQ, respiratory quotient; VO_2, oxygen consumption; WT, wild-type.

Materials and Methods

Generation of targeted mutant MCHR1−/− *mouse strains*

An 835-bp mouse *MCHR1* cDNA fragment was amplified from a mouse brain cDNA library (CLONETECH Laboratories, Palo Alto, CA) by PCR using two oligonucleotide primers (5′-GTCCCC-GACATCTTCATCATC-3′ and 5′-TCAGGTGCCTTTGCTTTCTGT-3′) designed from two homologous regions of the rat and human *MCHR1* genes. Using the murine *MCHR1* cDNA fragment as a probe, we isolated mouse genomic DNA clones corresponding to the *MCHR1* locus from mouse strain 129/SvJ [bacterial artificial chromosome (BAC) mouse embryonic stem library, Incyte Genomics Inc. (St. Louis, MO)]. A BAC clone was characterized by restriction mapping and two *Sca*I restriction fragments that span the entire coding region of the *MCHR1* gene were subcloned into a pZErO-1 vector (Invitrogen, San Diego, CA). A targeting vector backbone pGT-NN-tk was constructed by replacing the PGKneo cassette in pGT-N29-tk (21) with a neogene cassette from plasmid pKO SelectNeo (Lexicon Genetics Inc., Woodlands, TX) (Fig. 1A). The targeting vector pKOMCHR1 was constructed by inserting a 2.5-kb *Xho*I/*Eco*RI fragment that contains the 5′ promoter region and a 5.5-kb *Eco*RI/*Kpn*I

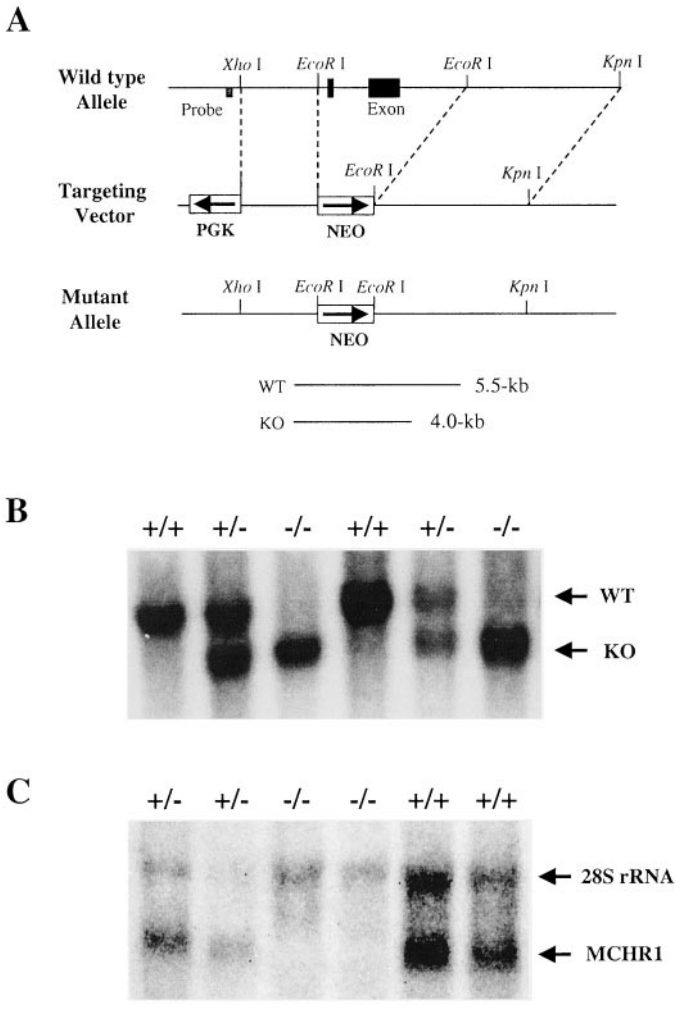

FIG. 1. Targeted disruption of the *MCHR1* gene in mice. A, *Top,* the targeted region of the *MCHR1* gene locus. *Middle,* The neocassette used to disrupt the entire coding region of the *MCHR1* gene. *Bottom,* The expected mutant allele with deletion of entire *MCHR1* gene. B, Southern blot analysis of mouse tail genomic DNA showed disappearance of 5.5-kb band in the *MCHR*−/− mice. Genotypes are shown at the *top.* C, Northern blot analysis of the mouse total brain RNAs indicated absence of *MCHR1* mRNA in the *MCHR1*−/− mice.

fragment that contains genomic sequences downstream from the 3′ untranslated region (Fig. 1A).

Plasmid pKOMCHR1 linearized with *Not*I was introduced into E14 mouse embryonic stem (ES) cells by electroporation. Selection of G418 and gancyclovir-resistant clones was performed as described (21). Genomic DNAs from transfectants were isolated and characterized by PCR. Clones carrying targeted disruption of the MCHR1 gene were identified by PCR using the following primers: ES3, 5′-GGAAGTAGCCTATAGGAAGAA-3′; pGKP1, 5′-CTCCAGACTGCCTTGGGAAAA-3′ and Elongase Enzyme mix from Life Technologies, Inc. (Rockville, MD; catalog no. 10480-010). The primer ES3 is located 60 bp upstream of the *Xho*I site in the 5′ promoter region of *MCHR1* and the primer pGKP1 is located in the neoselection marker. A 2.5-kb fragment was amplified from the genomic DNA of six ES clones with those reagents and Southern analysis confirmed homologous targeting events. Generation of chimeras was performed as described (21). Male chimeras were bred to female B6 mice to generate F1 heterozygous (*MCHR1*+/−) mice. Germline transmission of the *MCHR1* mutation to their F1 129/B6 offspring was identified by PCR and confirmed by Southern analysis of tail DNAs of agouti mice. F2 animals were maintained in sterilized microisolator cages and used for further analyses. All phenotypic study was performed on F2 129/B6 mice with 10–12 animals of each genotype [wild type (WT), heterozygous, and homozygous *MCHR1* deficient].

Mouse genotyping by PCR

Genotype analysis of large numbers of mice was facilitated by PCR. Two sets of primers were used in PCR to identify the presence of each allele. The following primer pairs lacked annealing site in the targeting vector and were used to detect WT allele: pair (A), WT1, 5′-TGTCAAGGGGATCCCTGCAGTC-3′; WT2, 5′-TGTGAGACCTTTCGAAAACGCTTGG-3′; and pair (B), WT3: 5′-GTCCCCGACATCTTCATCATC-3′; WT4, 5′-TCAGGTGCCTTTGCTTTCTGT-3′. The primer pairs for detection of mutant allele were: pair (A), pGKP1, 5′-CTCCAGACTGCCTTGGGAAAA-3′; KO1, 5′-CTCTGAGGCTACTGTCCATTCTA-3′; and pair (B), neo1, 5′-TTGGGAAGACAATAGCAGGC-3′, KO2, 5′-AGAGTTACAGAAGCAATGTA-3′. PCR was performed using the PCR supermix from Life Technologies, Inc. (catalog no. 10572-014), each primer of 200 nM and crude DNA extract from mouse tail in the final volume of 50 μl. The PCR samples were run on a 2% agarose gel to check for the presence or absence of an amplified band specific to each primer pair.

Southern blot, Northern blot, and real-time PCR analyses

We used a 262-bp DNA fragment as a probe for Southern blot analysis to detect correctly targeted ES cells and to confirm mouse genotypes (Fig. 1B). This probe is specific for a segment of the mouse genomic sequence upstream of the 5′-arm of the targeting vector. Targeted disruption of the *MCHR1* gene with the *PGK-neo* cassette introduced two additional *Pvu*II recognition sites. Consequently, the probe detected a *Pvu*II fragment 5.5 kb in length with the WT allele(s) and a 4.0-kb *Pvu*II fragment with the correctly targeted, mutant *MCHR1* allele(s). Southern blot analysis was carried out according to Sambrook *et al.* (22). Northern blot analysis was carried out using total RNA isolated from the brain. Brains were removed from decapitated 2-month-old male WT (+/+), heterozygous (+/−), and homozygous (−/−) mice and immediately frozen on dry ice until total RNAs were extracted from them by TRIzol Reagent (Life Technologies, Inc.). The 835-bp cDNA fragment initially used to identify the genomic BAC clone was used as a probe. Probes used for expression analysis of *MCH, NPY,* and *orexin* genes were amplified by primers (*MCH*: 5′-GTCTGGCTGTAAAACCTTACC-3′ and 5′-ACCAGCAGGTATCAGACTTGCC-3′; *NPY*: 5′-TCGTGTGTTTGGGCATTCTGG-3′ and 5′-GTCTTCAAGCCTTGTTCTGG-3′; *orexin*: 5′-CTGTCGCCAGAAGACGTGTTC-3′ and 5′-GCTAAAGCGGTGGTAGTTACGG-3′) based on the cDNA sequences of each gene, respectively). Probe used for *β-actin* gene expression analysis was purchased from CLONTECH Laboratories, Inc. Northern blot analyses were performed according to Sambrook *et al.* (22), and the same blot was stripped and reused for expression analysis of all the genes. Quantification of gene expression level from the Northern blots was carried out using phosphor imager and the expression level of each gene was normalized with the level of *β-actin*. Real-time PCR analyses were carried out using Taqman PCR amplifier equipped with ABI PRISM 7700 sequence detector (Perkin-Elmer Corp., Foster City, CA). Fifty nanograms total RNA equivalent cDNA was used for Taqman PCR. Each sample was run in duplicate, and the expression levels of *AgRP* and *proopiomelanocortin (POMC)* were normalized with that of *β-actin,* and then they were compared among *MCHR1* knockout, heterozygous, and WT group. The primer and probe sequences for the *β-actin* gene were 5′-CCGTGAAAAGATGACCCAGA-3′ and 5′-TACGACCAGAGGCATACAG-3′; probe: 5′-TTTGAGACCTTCAACACCCCA-3′. The primer and probe sequences for the *POMC* gene were 5′-GGCGTCTGGCTCTTCTCG-3′ and 5′-AGCAACCCGCCCAAGG-3′; probe: 5′-AGGTCATGAAGCCACCGTAACGCTTG-3′. The primer and probe sequences for the *AgRP* gene were 5′-GCTAGATCCACAGAACCGCG-3′ and 5′-AGCAGGACTCGTGCAGCCT-3′; probe: 5′-TCTCGTTCTCCGCGTCGCTGTGT-3′.

Animal care

All experiments were performed in F2 (129 X B6 background) mice. Mice were maintained on a 12-h light, 12-h dark cycle (lights on 2200–1000 h). The animals were weaned and individually housed at 3 wk of age. All mice had free access to water and received standard mouse chow

(Purina 5015 chow, Ralston Purina Co., St. Louis, MO). Mice used for experiments reported in Figs. 3–7 were switched to a high fat-chow (TD 95217, 40% calories from fat; Teklad, Madison, WI) at 4 wk of age. Mice were allowed 1 wk to acclimate to the environment. Body weight and food consumption was measured once a week at 0800 h from the fourth week after birth. All animal use in this study was conducted in compliance with approved institutional animal care and use protocols according to NIH guidelines (NIH Publication No. 86-23, 1985). Fat mass was analyzed by nuclear magnetic resonance using an Echo System (Houston, TX) instrument. Lean body mass was calculated by subtracting fat mass from total weight.

Indirect calorimetry

Twenty-four-hour energy expenditure and respiratory quotient (RQ) were measured by indirect calorimetry using an open-circuit Oxymax calorimetry system equipped with laser beam (Columbus Instruments International Corp., Columbus, OH) as previously described (23). Oxygen consumption (VO_2), carbon dioxide production (VCO_2), and physical activities were measured simultaneously for 16 animals. RQ is the ratio of carbon dioxide production to VO_2. Energy expenditure was calculated as the product of caloric value of oxygen and VO_2 per kilogram of body weight where caloric value of oxygen = 3.815 + 1.232*RQ (24). Total calories expended were adjusted to 24 h to determine daily fuel utilization. Daily caloric intake was calculated as: (mass of daily food intake in g) × (physiological fuel value of the diet in kcal/g). All data are expressed as mean ± SEM.

Statistical analyses

Mixed-effects repeated-measures ANOVA models were used to analyze the continuous efficacy data. Models included the fixed, categorical effects of treatment, time of observation, and treatment-by-time interaction. The unstructured (co)variance structure was used to model the within-mouse errors in the analyses. This was based on visual inspection of the pair-wise correlations between time points and careful consideration of all (co)variance structure options (*e.g.* autoregressive, toeplitz, and compound symmetric structures, with and without heterogeneous variances). The Kenward-Roders approximation was used to estimate degrees of freedom for all significance tests. The appropriate treatment-by-time interaction contrast was used to assess the magnitude and significance of treatment group differences at each time point. Analyses were implemented using a likelihood-based repeated measures approach (SAS PROC MIXED).

Results

Generation of MCHR1-deficient mice

To determine the physiological functions of MCHR1 *in vivo*, we generated mice deficient in *MCHR1* expression by homologous recombination in ES cells. We engineered a targeting vector to replace the entire *MCHR1* coding sequence with a neomycin resistance cassette (Fig. 1A). Two targeted mutant ES clones identified by PCR and confirmed by Southern blot were injected into C57BL/6 blastocysts and resulted in 12 male chimeric offspring that transmitted the disrupted *MCHR1* allele through the germline. Heterozygous mutant mice were intercrossed to generate homozygous mutants that were identified by PCR and confirmed by Southern blot analyses of genomic DNA (Fig. 1B). The null mutation of *MCHR1* was demonstrated by the absence of *MCHR1* expression, as determined by Northern analysis of mRNA isolated from brain of WT (+/+), heterozygous (+/−), and homozygous mutant mice (−/−) (Fig. 1C).

Body weight and fat mass of MCHR1 knockout mice

The *MCHR1*−/− mice used in the current studies were generated by intercross of *MCHR1*+/− mice. Among the different genotypes, *MCHR1*−/− mice were born at the predicted Mendelian ratios without any obvious phenotypic abnormality. We also set up independent breeding colonies outside our animal facility by crossing male and female *MCHR1*−/− mice to each other. Under the breeding program, more than 100 homozygous *MCHR*1 knockout mice have been generated so far. There is no phenotypic defect observed from these mice to date. Both genders are fertile and born with equal ratios. When fed a regular mouse chow, both male and female *MCHR1*−/− mice gained less weight than WT mice at 7 wk of age. The effect is more apparent in male *MCHR1* mice that had a significantly lower body weight and fat mass, compared with WT controls (Fig. 2).

We next investigated the response of *MCHR1*-deficient and heterozygous mice to a high-fat diet (TD95217, 40% fat by calories). Dietary fat content plays an important role in induction of obesity, and high-fat diets are often used to differentiate phenotypes of genetically manipulated mice from their WT controls (25). When fed a high-fat diet, the weight gain in *MCHR1*−/− mice was lower than the WT controls, which became more apparent at later age. Weight differences were more pronounced in male *MCHR1*−/− mice, which gained significantly less weight than the WT controls at 7 wk of age (Fig. 3). In comparison, the mean body weight of the female *MCHR1*−/− mice trailed the WT mice

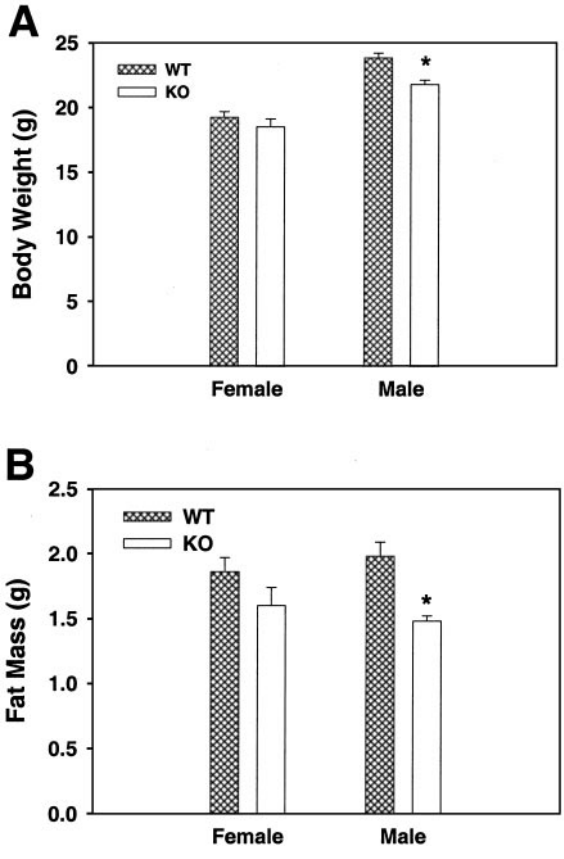

FIG. 2. Male, but not the female, *MCHR1* knockout mice fed regular chow had significantly lower body weight at 7 wk of age than the heterozygous and the WT controls. Data are the mean ± SEM of 11 mice per group. *, $P < 0.05$. WT represents the WT mice (*MCHR1*+/+) and KO represents the knockout mice (*MCHR1*−/−).

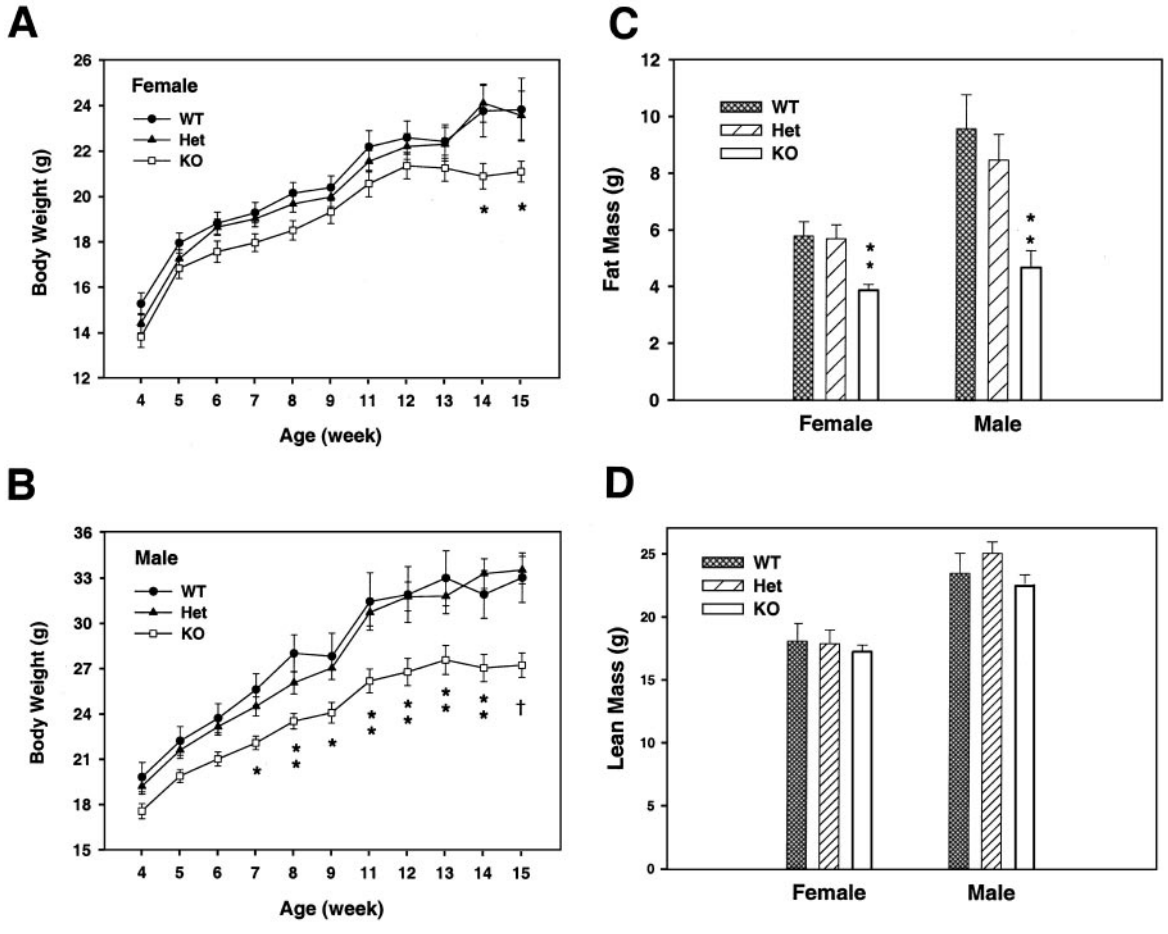

FIG. 3. Female and male *MCHR1* knockout mice fed high-fat diet had lower body weight (A and B) and fat mass (C and D) than their WT controls. Data are the mean ± SEM of 10 or 12 mice per group. *, $P < 0.05$; **, $P < 0.01$; †, $P < 0.001$, compared with WT group. WT, *MCHR1*+/+; Het, heterozygote (*MCHR1*+/−); KO, knockout (*MCHR1*−/−).

during the first few weeks of study and began to show significant differences at 14 wk of age. At 14 wk of age, male *MCHR1*−/− mice weighed 15% less and female *MCHR1*−/− mice weighed 12% less than the corresponding control mice. The body weight of the *MCHR1*+/− mice was indistinguishable from that of their WT controls throughout the studies. As measured by nuclear magnetic resonance, fat mass was decreased 30% and 50% in female and male *MCHR1*−/− mice, respectively, at 15 wk of age (Fig. 3C). Hence, the reduced body weight in both male and female *MCHR1*−/− mice was a consequence of decreased body fat mass. There was no significant difference in fat mass between WT and heterozygous mice. Reduced fat mass was not associated with any change in lean mass (Fig. 3D).

Consistent with a lower fat content, leptin levels were significantly lower in male but not in female *MCHR1*−/− mice, compared with the control mice measured at 15 wk of age (Fig. 4A). We next calculated leptin/fat ratio that can be used as an indicator for leptin sensitivity. When leptin levels were normalized to body fat for all three genotypes and both genders (nanogram per milliliter leptin per gram fat mass), there was a reduced leptin/fat ratio in the *MCHR1*−/− mice, but it did not reach statistical significance (females *MCHR1*+/+: 2.09 ± 0.52, *MCHR1*+/−: 2.18 ± 0.33, *MCHR1*−/−: 1.46 ± 0.13; males *MCHR1*+/+: 2.5 ± 0.52, *MCHR1*+/−: 1.87 ± 0.16, *MCHR1*−/−: 1.5 ± 0.11). As a result of fat mass reduction, significantly lower insulin levels were observed in both female and male *MCHR1*-deficient mice, compared with the corresponding control mice (Fig. 4B). Although lower insulin levels suggest improved insulin sensitivity, a more complete assessment of insulin sensitivity and glucose metabolism needs to be performed. There were no significant differences in plasma glucose levels between the *MCHR1*−/− mice (females: 192.09 ± 11.38; males: 225.2 ± 16.53 mg/dl) and the WT controls (females: 168.45 ± 7.43; males: 219.09 ± 16.78 mg/dl).

Decreased body mass and fat mass did not result from hypophagia. In fact, *MCHR1*−/− mice consumed more calories per unit weight on a daily basis. Food intake was increased by 15% in female *MCHR1*−/− mice, compared with controls (*MCHR1*−/−, 101.0 ± 2.3 g/kg of body weight; *MCHR1*+/+, 88.4 ± 4.2 g/kg of body weight; $P < 0.05$) (Fig. 5A) at 14 wk of age. The difference (20%) was greater in male *MCHR1*−/− mice, compared with WT mice (*MCHR1*−/−, 95.3 ± 4.7 g/kg of body weight; *MCHR1*+/+, 78.8 ± 2.6 g/kg of body weight, $P < 0.01$) (Fig. 5B) at 14 wk of age.

We next invested the fuel efficiency of the *MCHR1*-defi-

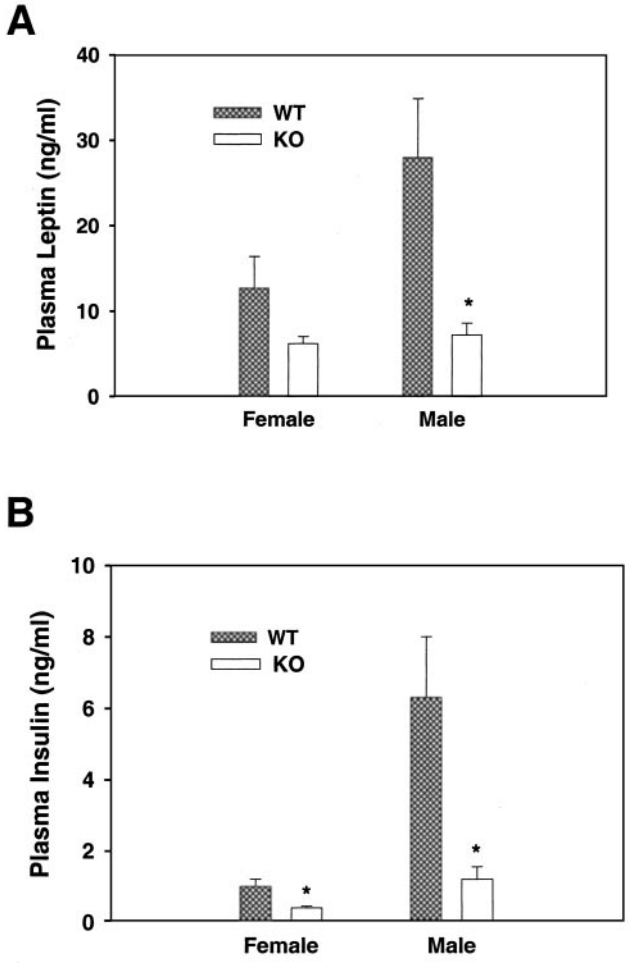

FIG. 4. Leptin (A) and insulin (B) levels of female and male *MCHR1* knockout mice fed high-fat diet at 15 wk of age. Data are the mean ± SEM of five mice/group. *, $P < 0.05$. WT represents the wild-type mice, and KO represents *MCHR1* knockout mice.

cient mice. Fuel efficiency has been calculated as body weight gain per kilocalorie food intake (mean ± SEM) of all the three genotypes of mice between 6 and 12 wk of age. As shown in Fig. 5C, male knockout mice had significantly lower fuel efficiency ($11.79 \pm 0.98 \times 10^{-3}$ g/kcal) than WT ($17.05 \pm 2.01 \times 10^{-3}$ g/kcal) and heterozygous mice ($18.06 \pm 1.06 \times 10^{-3}$ g/kcal) of the same gender, $P < 0.05$. However, fuel efficiency of female knockout mice ($8.48 \pm 0.64 \times 10^{-3}$ g/kcal) was not significantly different from WT ($9.22 \pm 0.91 \times 10^{-3}$ g/kcal) and heterozygous ($10.2 \pm 0.64 \times 10^{-3}$ g/kcal) mice.

Metabolic rate of MCHR1 knockout mice

To investigate whether the phenotype in *MCHR1*−/− mice results from changes in metabolic rate, indirect calorimetry was performed at 9–14 wk of age to study energy metabolism under high-fat diet. No significant differences in metabolic rate were observed between the *MCHR1*−/−-deficient and the WT controls in both male (Fig. 6A) and female mice (data not shown) over a 24-h period at 9 wk of age. Consistent with slower weight gain observed in male *MCHR1*−/− mice, total fuel utilization of the *MCHR1*−/− male mice increased sig-

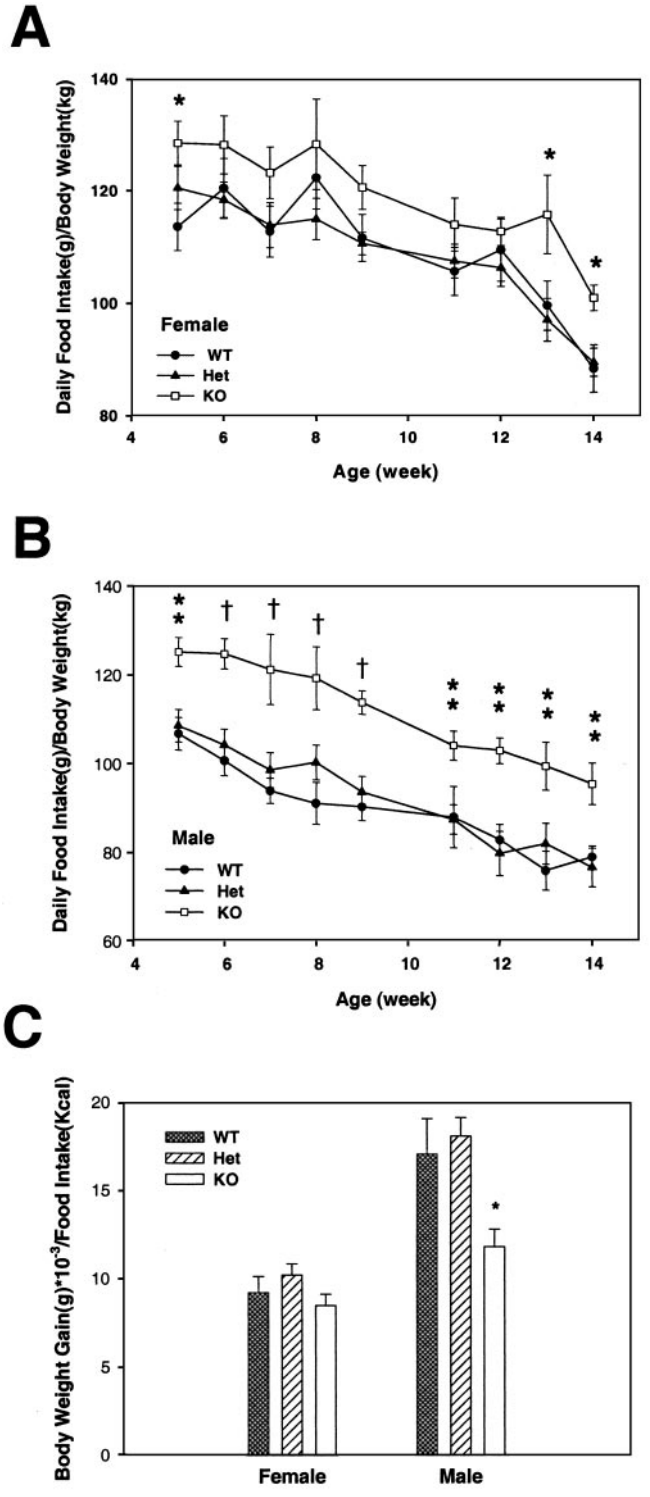

FIG. 5. Female and male *MCHR1* knockout mice fed high-fat diet had increased food consumption (A and B) and poor fuel efficiency (C). Food intake was expressed as daily food consumption divided by the corresponding body weight. Fuel efficiency was expressed as gram of body weight gain per kilocalorie food intake. Data are the mean ± SEM of 10 or 12 mice per group. *, $P < 0.05$; **, $P < 0.01$; †, $P < 0.001$, compared with WT group. WT, *MCHR1*+/+; Het, heterozygous (*MCHR1*+/−); KO, knockout (*MCHR1*−/−).

nificantly over a 24-h period at 11 wk (Fig. 6B) and 14 wk of age (data not shown). Total energy expenditure was 28% higher ($P < 0.05$) in male *MCHR1*−/− over a 24-h period at 11 and 14 wk of age when expressed as a percentage of the controls (Fig. 6C). In contrast, no significant differences were observed in females between the *MCHR1*−/− and the WT controls in total energy expenditure throughout the study period (Fig. 6C). Some of the extra energy expenditure could be due to increased activities because ambulatory movement was slightly increased in the male *MCHR1*−/− mice during a period when increased energy expenditure was observed. However, the difference was not significant (data not shown).

Changes in body weight and energy expenditure in response to fasting

We next investigated the response of *MCHR1*−/− mice to food deprivation at 15 wk of age. Following a 24-h fast, the male *MCHR1*−/− mice lost significantly more body weight, compared with the WT controls (Fig. 7A). Body weight loss was 7.4% in WT and 9.9% in *MCHR1* knockout animals,

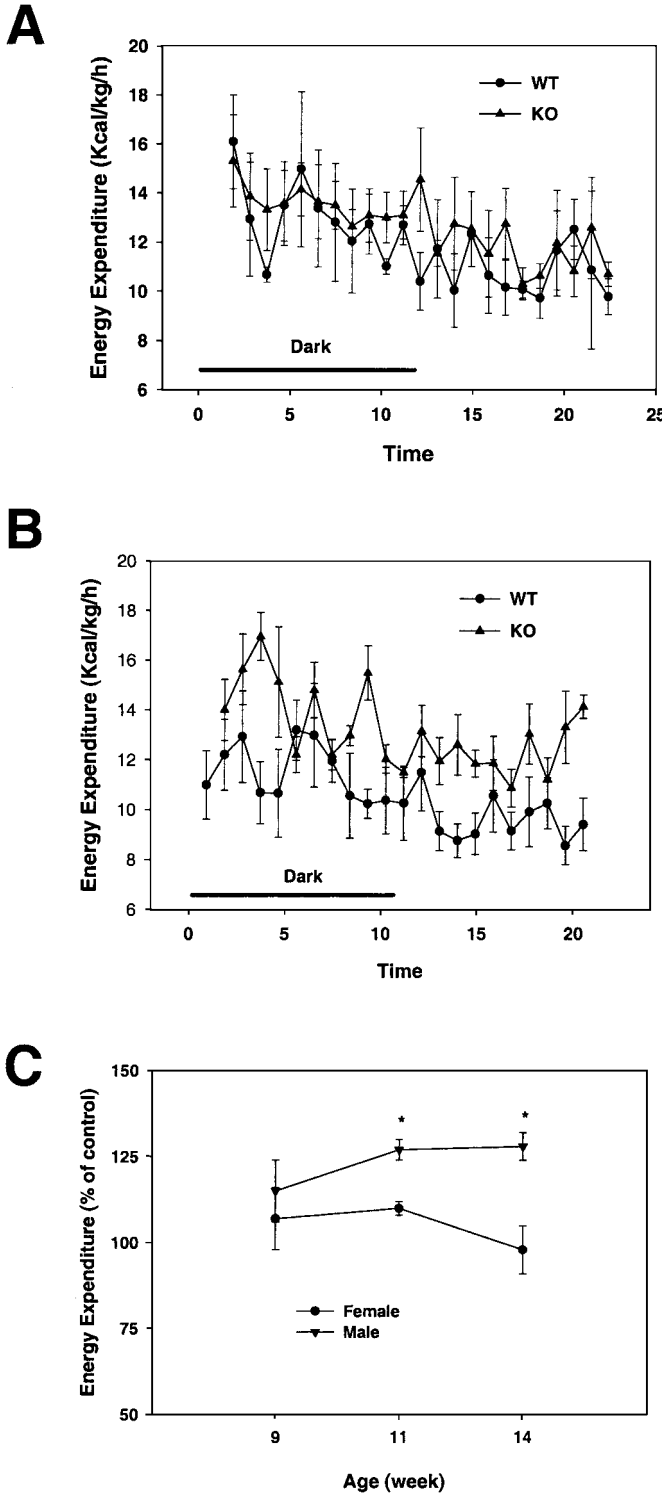

FIG. 6. Energy expenditure was increased in male knockout mice fed high-fat diet. Twenty-four-hour energy expenditure of male *MCHR1*+/+ and *MCHR1*−/− at wk 9 (A) and wk 11 (B). C, Summary of energy expenditure in female and male *MCHR*−/− mice, compared with corresponding WT group. Data are the mean ± SEM of five mice/group. *, $P < 0.05$, compared with WT group, which is 100.

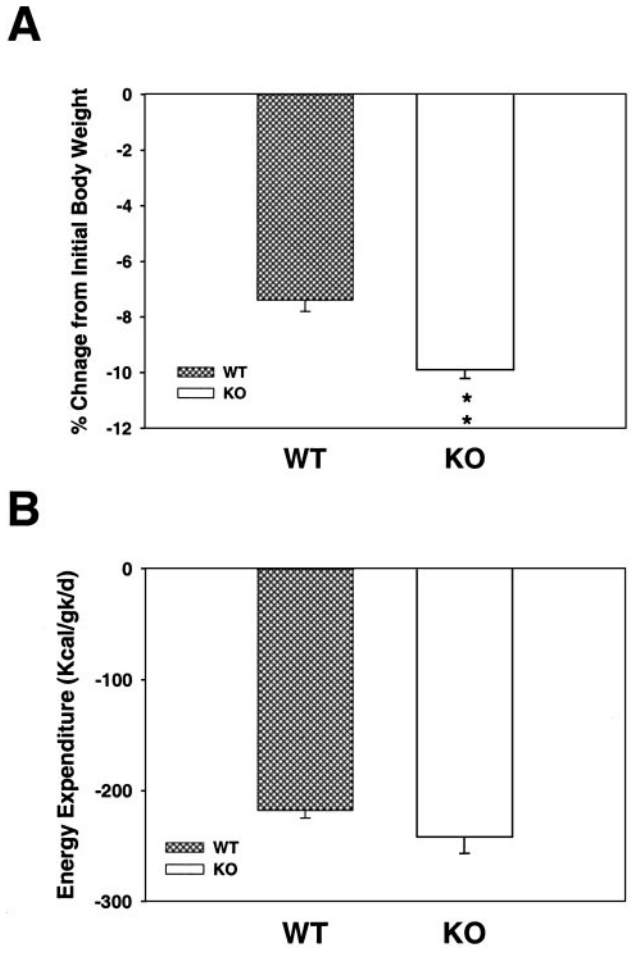

FIG. 7. Changes in body weight and energy expenditure in responses to fasting. A, Body weight reduction after 24-h fasting in male *MCHR1*−/− and *MCHR1*+/+ mice at 15 wk of age. B, Total energy expenditure during 24-h fasting in male *MCHR1*−/− and *MCHR1*+/+ mice. Data are the mean ± SEM of five mice per group. **, $P < 0.01$, compared with WT group.

compared with the prefast value. Despite the energy deficit caused by fasting, the total energy expenditure of male *MCHR1*−/− mice was 11% higher than that of WT mice (242 ± 15 *vs.* 218 ± 7 kcal/kg per day) (Fig. 7B), suggesting increased metabolic rate caused by *MCHR1* inactivation.

Effect of MCHR1 inactivation on expression of neuropeptide genes

Northern blot and quantitative PCR analyses were carried out on WT, heterozygous, and homozygous *MCHR1*-deficient mice to investigate possible feedback responses from other neuropeptides involved in energy balance. Northern blot analyses were carried out to study expression of *MCHR1*, *MCH*, *neuropeptide Y*, and *orexin* genes. The level of expression of each gene is quantified by phosphor imager and normalized with the expression level of *β-actin* that is used as internal control. Real-time PCR analyses were carried out to study the expression of both *AgRP* and *POMC* genes. As expected, there was no expression of the *MCHR1* gene in the knockout mice and a 50% reduction was observed in the heterozygous knockout mice, compared with the WT controls (Fig. 8). However, inactivation of the *MCHR1* gene did not alter the expression levels of *MCH*, *neuropeptide Y*, *orexin* (Fig. 8), *AgRP*, and *POMC* genes (data not shown). The results suggest that the metabolic pathway regulated by MCH is different from metabolic pathways induced by those neuropeptides (26).

Discussion

MCH has been implicated in a variety of physiological functions, in particular the regulation of energy homeostasis. Centrally administered MCH stimulates feeding, but MCH-deficient mice are hypophagic, lean, and hypermetabolic (4–6). These studies demonstrated a regulatory role of MCH in feeding and energy metabolism. Two recently identified human MCH receptors are expressed at high levels in the hypothalamic nuclei important for energy homeostasis (15–20). To understand the physiological role of each MCHR isoforms, particularly in regard to the regulation of energy metabolism, we generated *MCHR1*-deficient mice (*MCHR1*−/−). The *MCHR1*−/− mice were born at the expected Mendelian ratio confirming that the MCH pathway is not associated with embryonic or neonatal lethality (6).

Both male and female *MCHR1*−/− mice had a significantly reduced body weight, compared with WT littermates. However, male *MCHR1*−/− mice showed a reduced weight gain at a much earlier age (7 wk old), and a fat mass reduction of up to 50% was observed at 15 wk of age. In comparison, the lean mass was maintained at a level similar to that observed in the WT mice, suggesting that *MCHR1* inactivation did not cause pathophysiological weight loss such as muscle wasting. Despite increased food intake on a weight basis in the *MCHR1*-deficient mice, these mice were leaner than the heterozygous and the WT controls. This suggests that the decrease in weight gain is most likely because of an observed increase in metabolic rate in the *MCHR1*−/− animals. Consistent with the lower fat mass, both plasma leptin and insulin levels are significantly lower in male *MCHR1*-deficient mice than those from the WT controls. Although in both male and female *MCHR1*−/−mice, there was a reduced leptin/fat ratio, which is an indicator for leptin sensitivity, it did not reach statistical significance. While lower insulin levels often suggest improved insulin sensitivity, a more detailed metabolic study needs to be performed to confirm the effect. Even though the *MCHR1*-deficient mice experienced less

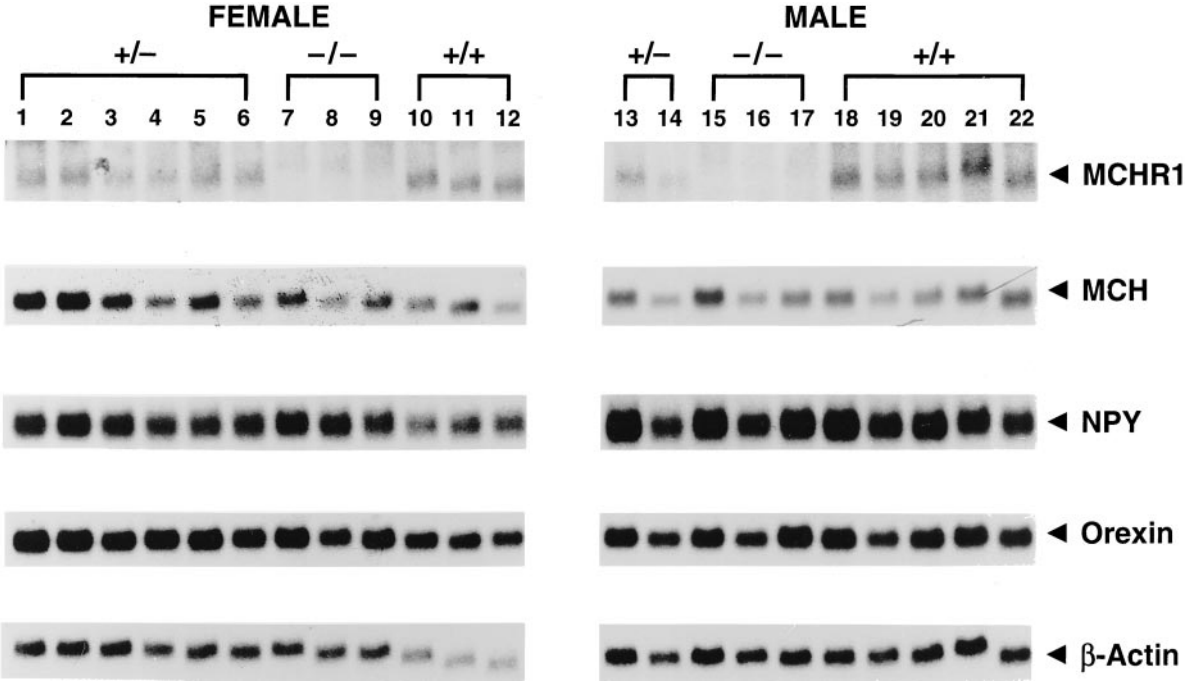

FIG. 8. Northern blot analysis of neuropeptide gene expression. The level of expression of each gene was quantified by phosphor imager and was normalized with the expression level of *β-actin*, which was used as internal control. The same blot was reused for analysis of all the genes.

positive energy balance because of poor fuel efficiency, there was no compensatory response in the MCH mRNA expression in the knockout mice. Similarly, no changes in mRNA levels were observed from other regulatory neuropeptides involved in energy balance, such as neuropeptide Y, orexin, AgRP, and POMC, suggesting that the metabolic pathway regulated by MCH is different from metabolic pathways induced by those neuropeptides (26).

Total fuel utilization is the sum of fuel used for basal processes, thermogenesis, and physical activities (27, 28). Daily fuel utilization of male *MCHR1*−/− mice was increased by 28% at 11 wk of age, compared with the WT controls. This is likely due to an increase in metabolic rate and physical activity. Indeed, we observed a slight increase in locomotion in male *MCHR1*−/− mice between 11 and 15 wk of age when energy expenditure was increased in *MCHR1*−/− mice (data not shown). Increased food intake in *MCHR1*−/− may also be a compensatory response to the hypermetabolic rate and poor fuel efficiency experienced in the male *MCHR1*-deficient mice. Thus, despite hyperphagia, the *MCHR1*−/− mice gain less fat mass than the WT mice. The recent observation that MCH inhibits the thyroid axis directly at the pituitary, which expresses MCHR1, may provide a possible mechanism for the hypermetabolic state (29). Although increased energy expenditure appears to be the mechanism contributing to reduced weight gain in the *MCHR1*−/− mice, it should be pointed out that early in the development of the phenotype significant reductions in body weight were seen in the absence of significant increases in energy expenditure. This likely is due to low sensitivity in measuring energy expenditure over a 24-h period and the fact that weight gain is an accumulative measurement over many weeks and is therefore less sensitive to daily fluctuation.

The phenotypic traits of *MCHR1*−/− mice generally reflect the phenotypes of *MCH*−/− mice, suggesting that MCH effects on fat storage and energy metabolism are primarily mediated by MCHR1. However, some phenotypic differences also exist between the *MCHR1*-deficient mice and the *MCH* knockout mice. Most notably, although both male and female *MCH*−/− mice are equally susceptible to weight reduction (6), *MCHR1* inactivation results in a more pronounced effect on reduction in mean body weight and fat mass in male *MCHR1*−/− mice than that in the females. Other phenotypic differences are less comparable between the *MCH*−/− and *MCHR1*−/− mice because of differences in diet used in the two studies. Nevertheless, it is noted that in contrast to hypophagia observed in the *MCH*−/− mice, the *MCHR1*−/− mice are hyperphagic. Because the phenotype of MCH knockout mice should be equivalent to inactivation of all the MCH receptors, these differences may be attributable to the effect of the newly identified MCHR2 whose physiological function remains to be investigated. Alternatively, it is noteworthy that the phenotype of the *MCH*−/− mice is complicated by deletion of sequences encoding the neuropeptides EI (NEI) and GE (6). Physiological functions of NEI and neuropeptide GE are poorly understood; however, both MCH and NEI have been shown to inhibit TRH release from hypothalamic explants (29). NEI has also been implicated in antagonizing effects of MCH on the hypothalamic-pituitary-adrenal axis (30). Nevertheless, our current work with the *MCHR1*-deficient mice has firmly established a role of MCH in regulating energy homeostasis. Moreover, our data demonstrate that MCHR1 plays an important role in energy homeostasis mediated by MCH.

In conclusion, we have generated *MCHR1* knockout mice and demonstrated that these mice are hyperphagic, hypermetabolic, and resistant to diet induced obesity. Our observations establish MCH as an important regulator of energy homeostasis; more importantly, inactivation of *MCHR1* alone is able to counterbalance obesity induced by a high-fat diet. The ongoing increase in the incidence of obesity and its associated susceptibility of type 2 diabetes has drawn attention in identifying novel and innovative treatments to counteract these epidemics. Identification, generation, and development of compounds that specifically antagonize MCHR1 may provide useful new medicines in treating and/or preventing human obesity.

Acknowledgments

We are grateful to Dr. Paul Burn for strong support and encouragement of this project. The authors also would like to thank Dr. Mark Farmen for help in statistical analysis and Drs. Paul Burn and Dana Sindelar for critical review of the manuscript.

Received January 31, 2002. Accepted March 18, 2002.

Address all correspondence and requests for reprints to: Dr. Yuguang Shi, Lilly Research Laboratories, Endocrine Division, Lilly Corporate Center, DC 0545, Eli Lilly & Co., Indianapolis, Indiana 46285. E-mail: shi_yuguang@lilly.com.

References

1. **Kawauchi H, Kawazoe I, Tsubokawa M, Kishida M, Baker BI** 1983 Characterization of melanin-concentrating hormone in chum salmon pituitaries. Nature 305:321–323
2. **Skofitsch G, Jacobowitz DM, Zamir N** 1985 Immunohistochemical localization of a melanin concentrating hormone-like peptide in the rat brain. Brain Res Bull 15:635–649
3. **Bittencourt JC, Presse F, Arias C, Peto C, Vaughan J, Nahon JL, Vale W, Sawchenko PE** 1992 The melanin-concentrating hormone system of the rat brain: an immuno- and hybridization histochemical characterization. J Comp Neurol 319:218–245
4. **Qu D, Ludwig DS, Gammeltoft S, Piper M, Pelleymounter MA, Cullen MJ, Mathes WF, Przypek R, Kanarek R, Maratos-Flier E** 1996 A role for melanin-concentrating hormone in the central regulation of feeding behaviour. Nature 380:243–247
5. **Rossi M, Choi SJ, O'Shea D, Miyoshi T, Ghatei MA, Bloom SR** 1997 Melanin-concentrating hormone acutely stimulates feeding, but chronic administration has no effect on body weight. Endocrinology 138:351–355
6. **Shimada M, Tritos NA, Lowell BB, Flier JS, Maratos-Flier E** 1998 Mice lacking melanin-concentrating hormone are hypophagic and lean. Nature 396:670–674
7. **Ludwig DS, Tritos NA, Mastaitis JW, Kulkarni R, Kokkotou E, Elmquist J, Lowell B, Flier JS, Maratos-Flier E** 2001 Melanin-concentrating hormone overexpression in transgenic mice leads to obesity and insulin resistance. J Clin Invest 107:379–386
8. **Jezova D, Bartanusz V, Westergren I, Johansson BB, Rivier J, Vale W, Rivier C** 1992 Rat melanin-concentrating hormone stimulates adrenocorticotropin secretion: evidence for a site of action in brain regions protected by the blood-brain barrier. Endocrinology 130:1024–1029
9. **Murray JF, Mercer JG, Adan RA, Datta JJ, Aldairy C, Moar KM, Baker BI, Stock MJ, Wilson CA** 2000 The effect of leptin on luteinizing hormone release is exerted in the zona incerta and mediated by melanin-concentrating hormone. J Neuroendocrinol 12:1133–1139
10. **Gonzalez MI, Baker BI, Wilson CA** 1997 Stimulatory effect of melanin-concentrating hormone on luteinizing hormone release. Neuroendocrinology 66:254–262
11. **Monzon ME, de Souza MM, Izquierdo LA, Izquierdo I, Barros DM, de Barioglio SR** 1999 Melanin-concentrating hormone (MCH) modifies memory retention in rats. Peptides 20:1517–1519
12. **Monzon ME, De Barioglio SR** 1999 Response to novelty after i.c.v. injection of melanin-concentrating hormone (MCH) in rats. Physiol Behav 67:813–817

13. **Chambers J, Ames RS, Bergsma D, Muir A, Fitzgerald LR, Hervieu G, Dytko GM, Foley JJ, Martin J, Liu WS, Park J, Ellis C, Ganguly S, Konchar S, Cluderay J, Leslie R, Wilson S, Sarau HM** 1999 Melanin-concentrating hormone is the cognate ligand for the orphan G-protein-coupled receptor SLC-1. Nature 400:261–265
14. **Saito Y, Nothacker HP, Wang Z, Lin SH, Leslie F, Civelli O** 1999 Molecular characterization of the melanin-concentrating-hormone receptor. Nature 400: 265–269
15. **Hervieu GJ, Cluderay JE, Harrison D, Meakin J, Maycox P, Nasir S, Leslie RA** 2000 The distribution of the mRNA and protein products of the melanin-concentrating hormone (MCH) receptor gene, slc-1, in the central nervous system of the rat. Eur J Neurosci 12:1194–1216
16. **Saito Y, Cheng M, Leslie FM, Civelli O** 2001 Expression of the melanin-concentrating hormone (MCH) receptor mRNA in the rat brain. J Comp Neurol 435:26–40
17. **Mori M, Harada M, Terao Y, Sugo T, Watanabe T, Shimomura Y, Abe M, Shintani Y, Onda H, Nishimura O, Fujino M** 2001 Cloning of a novel G protein-coupled receptor, SLT, a subtype of the melanin-concentrating hormone receptor. Biochem Biophys Res Commun 283:1013–1018
18. **Hill J, Duckworth M, Murdock P, Rennie G, Sabido-David C, Ames RS, Szekeres P, Wilson S, Bergsma DJ, Gloger IS, Levy DS, Chambers JK, Muir AI** 2001 Molecular cloning and functional characterization of MCH2, a novel human MCH receptor. J Biol Chem 276:20125–20129
19. **Sailer AW, Sano H, Zeng Z, McDonald TP, Pan J, Pong SS, Feighner SD, Tan CP, Fukami T, Iwaasa H, Hreniuk DL, Morin NR, Sadowski SJ, Ito M, Bansal A, Ky B, Figueroa DJ, Jiang Q, Austin CP, MacNeil DJ, Ishihara A, Ihara M, Kanatani A, Van der Ploeg LH, Howard AD, Liu Q** 2001 Identification and characterization of a second melanin-concentrating hormone receptor, MCH-2R. Proc Natl Acad Sci USA 98:7564–7569
20. **An S, Cutler G, Zhao JJ, Huang SG, Tian H, Li W, Liang L, Rich M, Bakleh A, Du J, Chen JL, Dai K** 2001 Identification and characterization of a melanin-concentrating hormone receptor. Proc Natl Acad Sci USA 98:7576–7581
21. **Liu JQ, Na SQ, Glasebrook A, Fox N, Solenberg PJ, Zhang Q, Song HY, Yang DD** 2001 Enhanced CD4(+) T cell proliferation and Th2 cytokine production in DR6-deficient mice. Immunity 15:23–34
22. **Sambrook J, Fritsch EF, Maniatis T** 1989 Molecular cloning: a laboratory manual. ed 2. Cold Spring Harbor, NY: CSH Laboratory Press
23. **Chen Y, Heiman ML** 2001 Increased weight gain after ovariectomy is not a consequence of leptin resistance. Am J Physiol Endocrinol Metab 280:E315–E322
24. **Elia M, Livesey G** 1992 Energy expenditure and fuel selection in biological systems: the theory and practice of calculations based on indirect calorimetry and tracer methods. World Rev Nutr Diet 70:68–131
25. **Asnicar MA, Smith DP, Yang DD, Heiman ML, Fox N, Chen YF, Hsiung HM, Koster A** 2001 Absence of cocaine- and amphetamine-regulated transcript results in obesity in mice fed a high caloric diet. Endocrinology 142:4394–4400
26. **Mystkowski P, Seeley RJ, Hahn TM, Baskin DG, Havel PJ, Matsumoto AM, Wilkinson CW, Peacock-Kinzig K, Blake KA, Schwartz MW** 2000 Hypothalamic melanin-concentrating hormone and estrogen-induced weight loss. J Neurosci 20:8637–8642
27. **Ravussin E, Danforth Jr E** 1999 Beyond sloth—physical activity and weight gain. Science 283:184–185
28. **Levine JA, Eberhardt NL, Jensen MD** 1999 Role of nonexercise activity thermogenesis in resistance to fat gain in humans. Science 283:212–214
29. **Kennedy AR, Todd JF, Stanley SA, Abbott CR, Small CJ, Ghatei MA, Bloom SR** 2001 Melanin-concentrating hormone (MCH) suppresses thyroid stimulating hormone (TSH) release, *in vivo* and *in vitro,* via the hypothalamus and the pituitary. Endocrinology 142:3265–3268
30. **Bluet-Pajot MT, Presse F, Voko Z, Hoeger C, Mounier F, Epelbaum J, Nahon JL** 1995 Neuropeptide-E-I antagonizes the action of melanin-concentrating hormone on stress-induced release of adrenocorticotropin in the rat. J Neuroendocrinol 7:297–303